Heterospin single-molecule magnets with extra-large anisotropic barrier

Yoshihara, Daisuke
Graduate School of Pharmaceutical Sciences, Kyushu University

Karasawa, Satoru
Graduate School of Pharmaceutical Sciences, Kyushu University

Koga, Noboru
Graduate School of Pharmaceutical Sciences, Kyushu University

出版情報：Polyhedron. 30 (18), pp.3211-3217, 2011-11-28. Elsevier
バージョン：

Manuscript Number: xxx

Heterospin Single-molecule Magnets with Extra-large Anisotropic Barrier

*Daisuke Yoshihara, Satoru Karasawa, and Noboru Koga**

† Graduate School of Pharmaceutical Sciences, Kyushu University, 3-1-1 Maidashi, Higashi-ku, Fukuoka, 812-8582 Japan,

*Corresponding author; tel +81 92 642 6590. Fax +81 92 641 6590
E-mail, koga@fc.phar.kyushu-u.ac.jp

ABSTRACT

The mixtures of Co(X-hfpip)$_2$; X = I and H, and bisdiazo-dipyridine ligands, **D2py$_2$(TBA)**, in 1:1 ratios gave the discrete cobalt complexes, **1** and **2**, respectively. The molecular structures for **1** and **2** revealed by X-ray crystallography were cyclic 2:2 cobalt complexes formulated as **[(Co(X-hfpip)$_2$)$_2$(D2py$_2$(TBA))$_2$]**, in which the cobalt units were compressed octahedra. After irradiation of the microcrystalline samples**,** the resulting Co-carbene complexes, **1c** and **2c**, showed SMM behaviors exhibiting slow magnetic relaxations. In dc and ac magnetic susceptibility experiments, the activation barrier, U_{eff}, for reorientation of the magnetic moment were estimated to be 139 and 135 K for **1c** and **2c**, respectively, and the hysteresis loops of the magnetization (the coercive force, H_c, and 26 and 15 kOe at 1.9 K for **1c** and **2c**, respectively) were observed. In addition, the values of the quantum tunneling time, τ_Q, were determined to be 1.1 x 10^5

and 5.4 x 10^5 sec ($t_{1/2}$ = 21 and 104 hours) for **1c** and **2c**, respectively, below 2.5 K.

Keywords: heterospin system, single-molecule magnet, cobalt(II) complex, carbene, hysteresis loop.

1. Introduction

A topic of current interest regarding single-molecule magnets (SMM) [1] in the field of the molecule-based magnet is the construction of SMM with a high effective activation barrier, U_{eff}, for reorientation of the magnetic moment.[2] An SMM with a large U_{eff} value leading to a high blocking temperature, T_B, below which the molecule becomes a magnet, is anticipated as a next-generation functional material, a nm-size magnet. In SMM, the characteristic slow magnetic relaxation for reorientation of the magnetic moment takes place via two pathways due to the thermal activation barrier U corresponding to $|D|S^2$, where $|D|$ ($D < 0$) is a uniaxial anisotropic parameter and S is a spin quantum number, and the quantum tunneling of the magnetization (QTM) [3] relating to the transverse anisotropic parameter, E. To obtain a large value of U_{eff} ($U > U_{eff}$), therefore, an increasing U value and/or a suppressing QTM pathway are required. Based on the strategy of the heterospin system [4] consisting of organic spins and metal ions, we have prepared heterospin SMMs [5] with relatively large U_{eff} values. Recently, a cyclic 2:2 complex, **[(Co(*tert*-Bu-hfpip)$_2$)$_2$(D2py$_2$(TBA))$_2$]**, composed of the cobalt complex, **Co(*tert*-Bu-hfpip)$_2$**; bis{1, 1, 1, 5, 5, 5, hexafluoro-4-(4-*tert*-butylphenylimino)-2-pentanonate}cobalt and photoresponsive magnetic coupler, **D2py$_2$(TBA),** was found to be photolyzable in the crystalline state and exhibited an SMM behavior with U_{eff} = 96 K and H_c = 10 kOe at 1.9 K after irradiation and then annealing at 70 K. [6] To alterate the local circumstance of cobalt ions in this heterospin system, this time, diazo-substituted Co(hfpip)$_2$ complexes, **[(Co(X-hfpip)$_2$)$_2$(D2py$_2$(TBA))$_2$]**; **X** = **H**, **I**, **Br**, **NO$_2$** and **CF$_3$**, were prepared and the substituent effects of the hfpip cobalt complexes on the SMM magnetic properties were investigated. In these complexes, we found the iodo and no substituent complexes, **[(Co(I-hfpip)$_2$)$_2$(D2py$_2$(TBA))$_2$]**, **1**, and **[(Co(hfpip)$_2$)$_2$(D2py$_2$(TBA))$_2$]**, **2**, exhibiting SMM behaviors with extra-large anisotropic barriers after irradiation. Interestingly, in these complexes, the temperature-independent magnetization decays due to QTM were

observed in 2.5 – 1.9 K. In this paper, we reported the molecular structures of **1** and **2**, their SMM behaviors after irradiation, and the comparison of the SMM properties with that for **[(Co(*tert*-Bu-hfpip)$_2$)$_2$(D2py$_2$(TBA))$_2$]**, **3**, reported previousely [6].

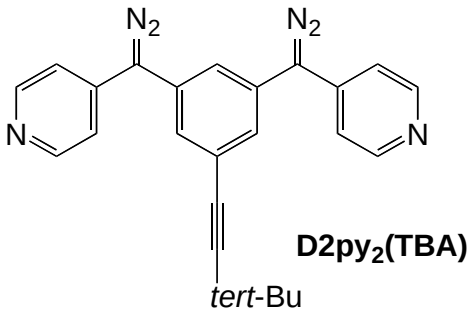

D2py$_2$(TBA)

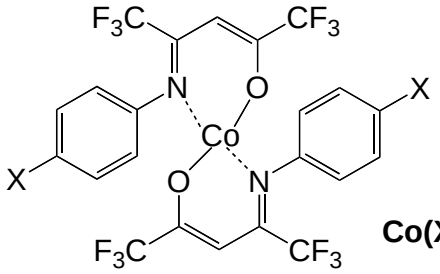

Co(X-hfpip)$_2$

[Co(X-hfpip)$_2$(D2py$_2$(TBA))$_2$]
1; X = I, **2**; X = H, **3**; X = *tert*-Bu

2. Experimental

2.1. General

Infrared spectra were recorded on a JASCO 420 FT-IR spectrometer. Melting points were obtained with a MEL-TEMP heating block and are uncorrected. Elemental analyses were performed in the Analytical Center of the Faculty of Science in Kyushu University.

2.2. X-ray Crystal and Molecular Structure Analyses

Crystallographic data and experimental details for **D2py$_2$(TBA)**, **1**, and **2**, are summarized in Table 1. Suitable single crystals were glued onto a glass fiber using epoxy resin. All X-ray data were collected on a Rigaku Raxis-Rapid diffractometer with graphite monochromated MoK$_\alpha$ radiation (λ = 0.71069 Å). Reflections were collected at 123 ± 1 K. The molecular structures were solved by direct methods (SIR program) and expanded using Fourier techniques (DIRDIF94). The refinements were converged using the full-matrix least squares method from the Crystal Structure software package [7] to give the *P*-1 (no. 2) for **D2py$_2$(TBA)**, **1**, and **2**. All non-hydrogen atoms were refined anisotropically, hydrogen atoms were included at standard positions (C-H = 0.96

Å, C-C-H = 120 °) and refined isotropically using a rigid model. Crystallographic data for the structure reported in this paper have been deposited with the Cambridge Crystallographic Data Center as supplementary publication no. CCDC-803425, 734081, and -803858 for **D2py$_2$(TBA)**, **1**, and **2**, respectively.

Table 1

Crystallographic data of **D2py$_2$(TBA)**, **1**, and **2**

	D2py$_2$(TBA)	**1**	**2**
empirical formula	$C_{24}H_{20}N_6$	$C_{92}H_{60}F_{24}N_{16}O_4I_4Co_2$ /4CH_2Cl_2/2CH_3CN	$C_{92}H_{64}N_{16}O_4F_{24}Co_2$ /4CH_2Cl_2
Formula Weight	392.46	2956.87	2201.29
Crystal system	triclinic	triclinic	triclinic
Space group	*P*-1 (no 2)	*P*-1 (no 2)	*P*-1 (no 2)
a (Å)	8.886(8)	13.436(4)	11.807(10)
b (Å)	11.036(9)	14.523(5)	12.568(10)
c (Å)	11.845(11)	15.858(4)	18.450(15)
α (deg)	77.998(3)	90.201(11)	106.541(10)
β (deg)	70.511(3)	104.302(11)	90.228(10)
γ (deg)	70.025(3)	104.926(13)	91.988(10)
V (Å^3)	1023(16)	2890(14)	2623(4)
μ (cm^{-1})	0.794	16.363	6.202
Z	2	1	1
crystal size (mm)	0.80×0.50×0.20	0.40×0.40×0.30	0.30×0.30×0.20
D_{calc} (gcm^{-3})	1.274	1.699	1.501
Color	Red	Red	Red
F (000)	412.00	1247.00	1198.00
radiation	Mo-K_α	Mo-K_α	Mo-K_α
R_1, wR_2 [$I > 2\sigma(I)$]	0.062, 0.196	0.068, 0.212	0.067, 0.192
GOF	1.102	1.120	1.052
No of obs.	4596	29271	9214
No of variables	272	722	740

[a] $R_1 = \Sigma\, ||F_0|-|F_c|| / \Sigma\, |F_0|$; $wR_2 = \{ \Sigma\, w(F_0^2-F_c^2)^2 / \Sigma\, w(F_0^2)^2 \}^{1/2}$

2.3. Measurements and Analyses of Magnetic Properties

Direct current (dc) and alternating current (ac) magnetic susceptibility data were obtained on a Quantum Design MPMS5S SQUID magneto/susceptometer, and corrected for the magnetization of the sample holder and capsule, and for diamagnetic

contributions to the samples, which were estimated from Pascal's constants [8]. The concentrations of the starting diazo-cobalt complexes were used as those of the samples after irradiation. Ac magnetic susceptibility measurements were carried out with a 3.9 Oe oscillating field and a zero dc field at a frequency of 1 - 997 Hz. Photolyses of the samples were performed inside a sample room of SQUID by using the irradiation system reported previously [4].

2.4. Materials

Bisdiazo-dipyridyl ligand, **D2py$_2$(TBA)**, and the cobalt complexes, **Co(X-hfpip)$_2$**; **X** = **I** and **H**, were prepared by the procedure reported previously. [6, 9]

D2py$_2$(TBA); Solutions of **D2py$_2$(TBA)** in CH_2Cl_2 and CH_3CN were kept at 4 °C to afford the single crystals as of red bricks. m.p. (dec.) 126 °C, IR (KBr disck.) 2049 cm^{-1}, Anal. Calcd for $C_{24}H_{20}N_6$: C 73.45, H 5.14, N 21.41; found: C 73.16, H 5.10, N 21.34.

[(Co(I-hfpip)$_2$)$_2$(D2py$_2$(TBA))$_2$], **1**; Solutions of diazo-dipyridine ligand **D2py$_2$(TBA)**$_2$ (32 mg, 0.08 mmol) in CH_2Cl_2 (4 mL) and cobalt complex **Co(I-hfpip)$_2$** (70 mg, 0.08 mmol) in CH_3CN (4 mL) were mixed and kept at 4 °C. The 2:2 cobalt(II) complex, **1**, was obtained as single crystals of dark red bricks. m.p. (dec.) 153 °C, IR (KBr disck.) 2058 cm^{-1}, Anal. Calcd for $C_{92}H_{60}F_{24}N_{16}O_4Co_2/0.5CH_2Cl_2$: C 43.59, H 2.39, N 8.84; found: C 43.52, H 2.44, N 8.82.

[(Co(hfpip)$_2$)$_2$(D2py$_2$(TBA))$_2$], **2**; Solutions of diazo-dipyridine ligand **D2py$_2$(TBA)** (30 mg, 0.08 mmol) in CH_2Cl_2 (4 mL) and cobalt complex Co(hfpip)$_2$ (48 mg, 0.08 mmol) in *n*-hexane (4 mL) were mixed and kept at 4 °C. The 2:2 cobalt(II) complex, **2**, was obtained as single crystals of dark red bricks. m.p. (dec.) 142 °C, IR (KBr disck.) 2058 cm^{-1}, Anal. Calcd for $C_{92}H_{64}F_{24}N_{16}O_4Co_2/0.5CH_2Cl_2$: C 54.39, H 3.18, N 11.03; found: C 54.51, H 3.17, N 11.03.

3. Results and Discussion

*3.1. X-ray Molecular Structure Analysis of **D2py$_2$(TBA)**, [Co(I-hfpip)$_2$(D2py$_2$(TBA))$_2$], **1**, and [Co(hfpip)$_2$(D2py$_2$(TBA))$_2$], **2***

The single crystals of **D2py$_2$(TBA)**, [Co(I-hfpip)$_2$(D2py$_2$(TBA))$_2$], **1**, and [Co(hfpip)$_2$(D2py$_2$(TBA))$_2$], **2** were analyzed by X-ray crystallography.

(A) ***D2py$_2$(TBA)***

ORTEP drawing of the molecular structure is shown in Fig. S1. Two diazo moieties in a molecule direct opposite direction and the dihedral angles between the benzene plane and the pyridine plane are 49.0 and 63.5 °, respectively.

(B) [Co(I-hfpip)$_2$(D2py$_2$(TBA))$_2$], ***1****, and [Co(hfpip)$_2$(D2py$_2$(TBA)) $_2$],* ***2***

The single crystals contained four CH_2Cl_2 and two CH_3CN molecules for **1** and four CH_2Cl_2 molecules for **2** used for the recrystallization. Complexes, **1** and **2**, were crystallized in the *P*-1 space group and both complexes and **3** were isomorphous with similar bond lengths and angles. The molecules of **1** and **2** had one symmetry center at the center of the cyclic molecule and the latter showed the disorders at C(20)-*tert*-butyl groups and diazo (N2-N3) moieties. In the molecular structure, two **D2py$_2$(TBA)**s bridged two **Co(X-hfpip)$_2$** by cis coordination to form a cyclic dinuclear complex. ORTEP drawings of molecular structure for **1** and **2** are shown in Fig. 1.

(a)

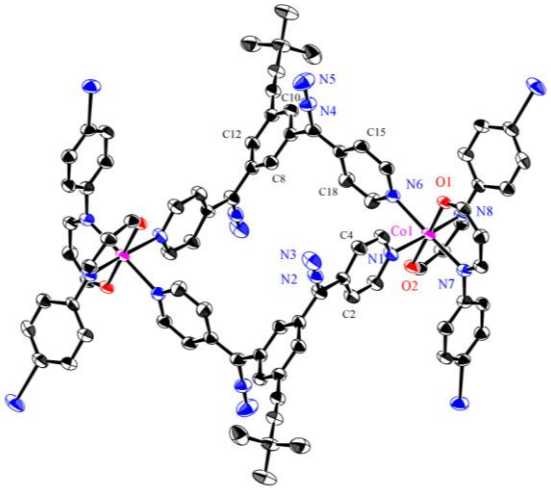

(b)

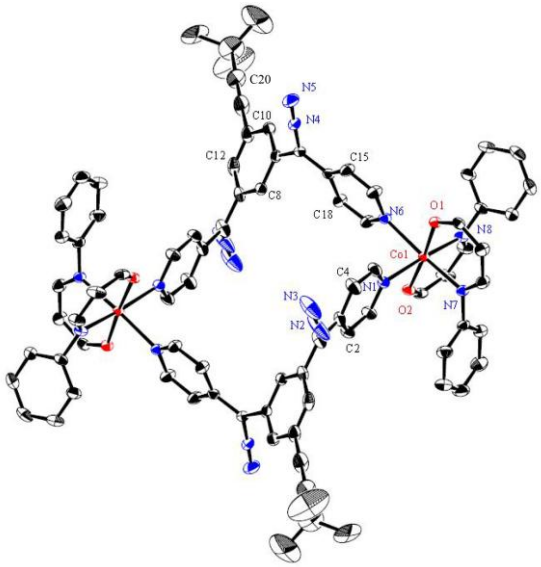

Fig. 1. ORTEP drawings of the molecular structure of **1** (a) and **2** (b) (C; black, N; blue, O; red, and Co; pink). Solvent molecules, trifluoromethyl, and hydrogen atoms are omitted for the sake of clarity.

The local structure of the cobalt ion unit is a compressed octahedron in which the bond lengths between the cobalt ion and the axial ligands (Co–O1 and O2) are shorter by 0.13 - 0.18 Å and 0.15 - 0.18 Å for **1** and **2**, respectively, than the others. The dihedral angles between the pyridine plane and the X-Y plane defined by four atoms coordinating to the cobalt ion are 73.22 and 81.16° for **1** and 75.18 and 80.11° for **2**. In bridging ligand, **D2py$_2$(TBA)**, diazo moieties direct opposite direction and the dihedral angles between the pyridine ring and the phenyl ring are 56.4 and 62.1 ° for **1** and 53.4 and 56.9 ° for **2**. These angles were consistent with those (49.0 and 63.5 °, Fig. S1) for free **D2py$_2$(TBA)**, indicating that **1** and **2** have no strain caused by the complexation with Co(X-hfpip)$_2$. The intramolecular Co–Co distances are 12.37 Å and 11.90 Å for **1** and **2**, respectively. No significant intermolecular short contacts were observed within 6 Å in the crystal packing (Fig. S2). Selected bond lengths and dihedral angles for **1** and **2** together with those for **3** are summarized in Table 2. Noticable difference of the moleculer structures in three complexes, **1**, **2**, and **3**, was observed in the dihedral angle between the pyridine plane and the X-Y plane. In **3**, the those angles are 80.26 and 62.55 ° and the second value is small compared with the first one and those for the correspinding angles in **1** and **2**. The observed small dihedral angle might reduce the magnetic interaction between the cobalt ion and the carbene generated by photolysis.

Table 2.

Selected Bond Lengths (Å) and Dihedral Angles (°) for **1**, **2**, and **3**

	1	**2**	**3**[a]
Bond Lengths (Å)			
Co-N(1)	2.161	2.190	2.206
Co-N(6)	2.182	2.186	2.167
Co-N(7)	2.206	2.181	2.192
Co-N(8)	2.176	2.182	2.170
Co-O(1)	2.026	2.027	2.011
Co-O(2)	2.030	2.014	2.028
Co-Co	12.37	11.90	11.31
Dihedral Angles (°) between Pyridine Ring and XY Plane			
N(1)N(6)N(7)N(8) -N(1)C(2)C(4)	73.22	80.11	80.26
N(1)N(6)N(7)N(8) -N(6)C(15)C(18)	81.16	75.18	62.55
Dihedral Angles (°) between Pyridine Ring and phenyl ring			
N(1)C(2)C(4) -C(8)C(10)C(12)	56.39	56.92	54.55
N(6)C(15)C(18) -C(8)C(10)C(12)	62.12	53.40	55.88

[a] ref [6]

3.2. Magnetic properties

*3.2.1. Photolyses of microcrystalline samples of **1** and **2***

Crystalline **1** and **2** (ca. 0.5 mg) ground and spread on cellophane tape were used as samples. Photolyses of the samples were performed in the sample room of SQUID apparatus through an optical fiber using light from an argon ion laser at λ = 514 nm below 10 K. The progress of photolysis was followed by M measurement at the constant field of 5 kOe and at 5 K. On photolysis, the M value for photoproducts, **1c** and **2c**, steeply increased and reached a saturation value after irradiation for 20 - 36 hrs. The

plot of *M* vs. *time* for **1** is shown in Fig. 2. The yields of photolysis of **1** and **2** were determined to be ca. 85 and 82 %, respectively, from the disappearance of the IR absorption at 2058 cm^{-1} due to the diazo moieties in the complex after SQUID measurements.

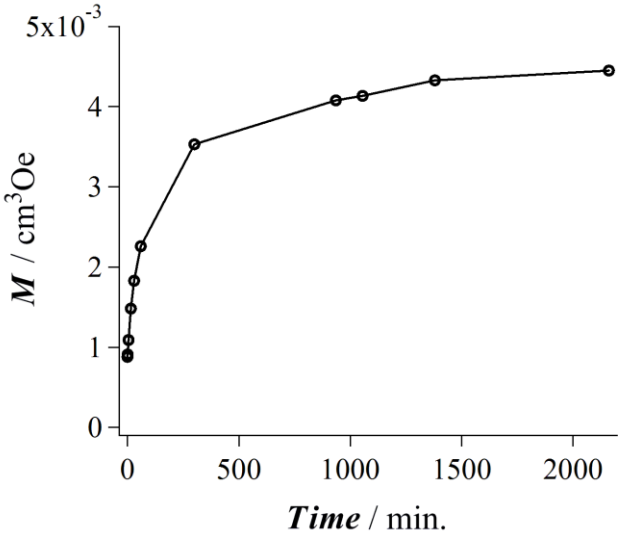

Fig. 2. Plot of *M* vs. irradiation time for **1** at ca. 5 K

3.2.2. Dc magnetic susceptibility measurements

The values of dc molar magnetic susceptibility, χ_{mol}, before and after irradiation of **1** and **2** were collected at the constant field of 5 kOe below 30 K. Obtained χ_{mol} values were plotted in a fashion of $\chi_{mol}T$ vs. T plot, as shown in Fig. 3. Before irradiation, the $\chi_{mol}T$ values in the $\chi_{mol}T$ vs. T plot were nearly constant (4.0 cm^3Kmol^{-1}) in the temperature range of 1.9–10 K. After irradiation, the $\chi_{mol}T$ values for **1c** were nearly constant (29 cm^3Kmol^{-1}) for 15 – 30 K and gradually decreased below 8 K (Fig. 3). Complex **2c** also showed a similar thermal profile of $\chi_{mol}T$ in $\chi_{mol}T$ vs. T plot and a constant $\chi_{mol}T$ value of 24 cm^3Kmol^{-1} was obtained (Fig. S3). These constant values are much larger than that (10.0 cm^3Kmol^{-1}) calculated by a spin-only equation with two isolated quintet carbenes (3.0 cm^3Kmol^{-1} x 2) and two high-spin cobalt(II) ions with effective spin S_{eff} = 1/2 ($\chi_{mol}T$ value of 4.0 cm^3Kmol^{-1} before irradiation) [8, 10], suggesting that the carbenes and the cobalt ions in the complex interacted ferromagnetically to form a high-spin ground state with S_{total} = 10/2. The decrease in the

$\chi_{mol}T$ values for both complexes below 8 K indicates an effect of the zero-field splitting caused by spin-orbit coupling in the cobalt ion.

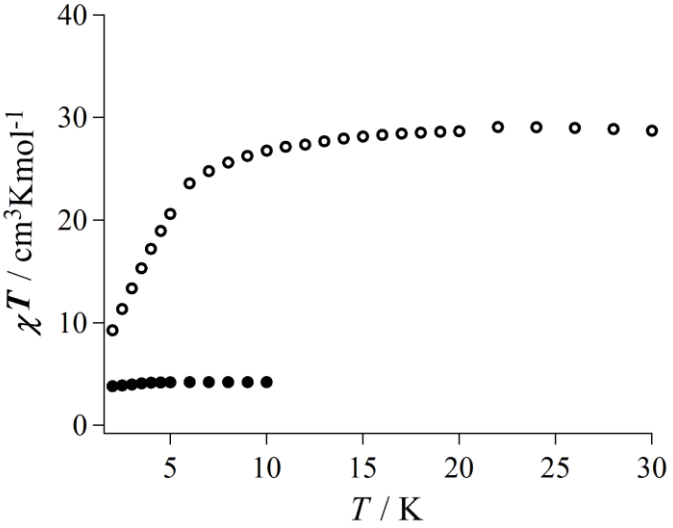

Fig. 3. Plots of $\chi_{mol}T$ vs T before (filled) and after irradiation (open) of **1.**

The field dependencies of dc magnetization, M_{mol}, for **1c** and **2c** were measured in the range –50 to +50 kOe with a field-sweep rate of 0.35 kOe/sec at the various temperatures below 6 K. The M_{mol} vs. H plots at various temperatures below 6 K for **1c** and **2c** are shown in Fig. 4.

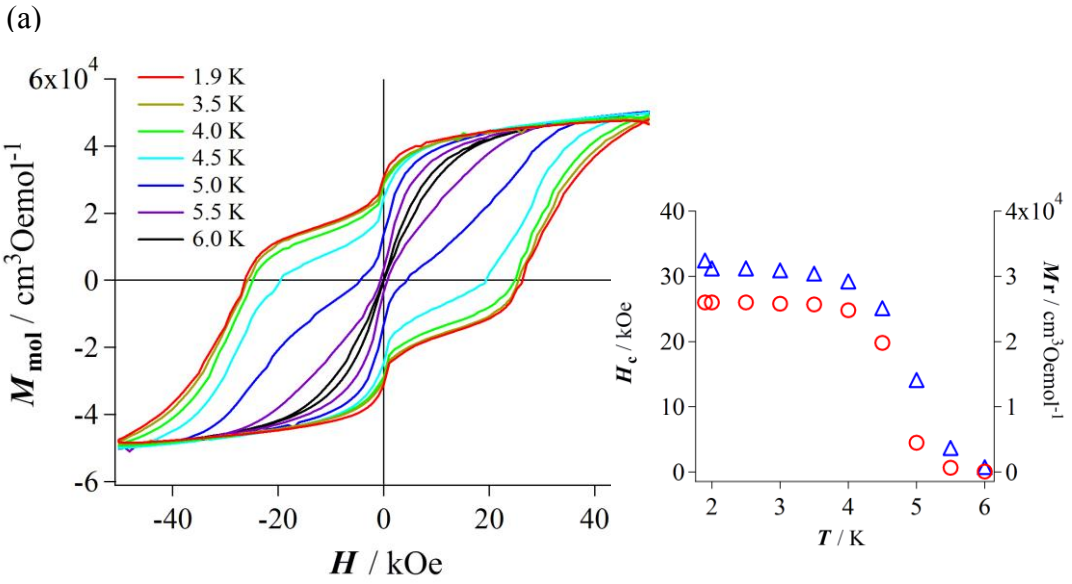

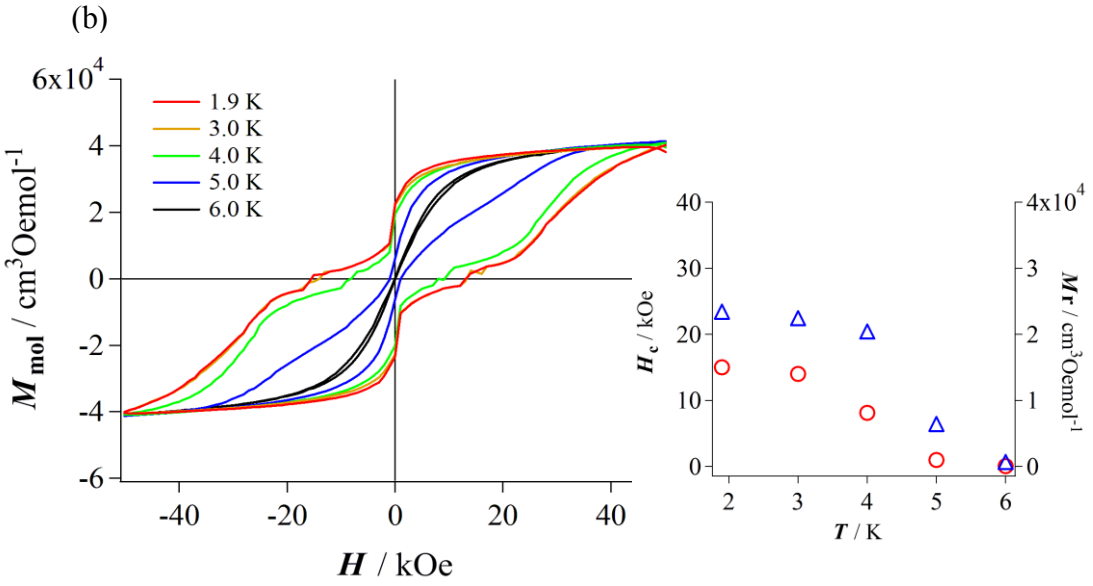

Fig. 4. Hysteresis loops of **1c** (a) and **2c** (b) at various temperatures in the range of 6.0 – 1.9 K. The field-sweep rate is 0.35 kOe/sec. The insets show the plots of H_c (○) and M_r (△) vs. T.

The M_{mol} values at 50 kOe for **1c** and **2c** were 4.6 x 10^4 and 4.0 x 10^4 cm^3Oemol^{-1}, which were still below the saturation magnetization, M_s. As observed in Fig. 4, the temperature-dependent hysteresis loops relating to the field appeared below ca. 6 K and anomalous changes (steps) of the M_{mol} values were observed at 0 and 29 kOe for **1c** and 0 and 27 for **2c** below 3 K. The observed field and temperature dependencies of M_{mol} were typical behaviors for SMM. The values of the coercive force, H_c, and the remnant magnetization, M_r, were plotted as a function of temperature (inset of Fig. 4). In the H_c vs. T plot, the coercive force appeared at ca. 6 K, increased on cooling, and reached a plateau below 3 K. The M_r vs. T plot also showed a similar thermal profile. The values of H_c, and the remnant magnetization, M_r, at 1.9 K were 26 kOe and 3.1 x 10^4 cm^3Oemol^{-1} for **1c** and 15 kOe and 2.3 x 10^4 cm^3Oemol^{-1} for **2c**.

*3.2.3. Magnetic Relaxation of **1c** and **2c***

In the magnetic relaxations due to U_{eff} and QTM, the former are temperature-dependent and obtained by the ac magnetic susceptibility technique, while the latter are

temperature-independent and determined by the temperature dependence of the dc magnetization decay at low temperature. To determine both relaxations, therefore, the ac and dc magnetic susceptibility measurements were carried out after irradiation of **1** and **2**.

*3.2.3.1. Ac magnetic susceptibility measurements for **1c** and **2c***

Ac magnetic susceptibility measurements at a zero dc field with a 3.9 Oe ac field were carried out in the temperature range of 1.9 - 14 K. Before irradiation, no χ''_{mol} signals (out-of-phase signal) were observed, while after irradiation, well-resolved χ'_{mol} (in-phase signal) and χ''_{mol} signals with frequency dependence were observed. The $\chi'_{mol}T$ vs. T and χ''_{mol} vs. T plots are shown in Fig. 5. In $\chi'_{mol}T$ vs. T plot, the $\chi'_{mol}T$ values at each frequency were constant by 30 and 24 cm^3Kmol^{-1} for **1c** and **2c**, respectively, until the temperature χ''_{mol} signals appeared and then decreased below it. The constant values were consistent with those (29 and 24 cm^3Kmol^{-1} for **1c** and **2c**, respectively) for $\chi_{mol}T$ in $\chi_{mol}T$ vs. T plots (Fig. 3). As observed in Fig. 5b and 5d, χ''_{mol} signals at each frequency showed a maximum above 6 K and the peak-top temperature shifted lower as the frequency decreased. The observations of χ''_{mol} signals with frequency dependence indicate that the complexes **1c** and **2c** have a slow magnetic relaxation for reorientation of the magnetic moment.

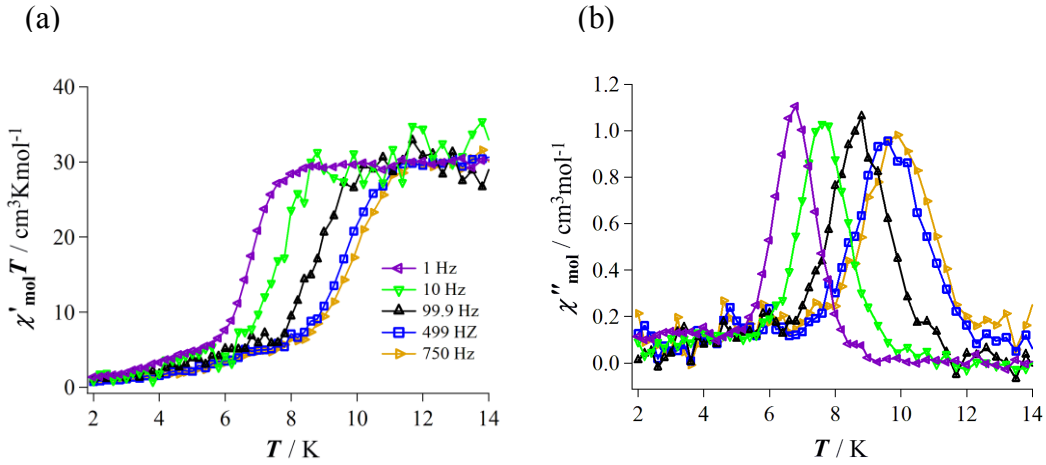

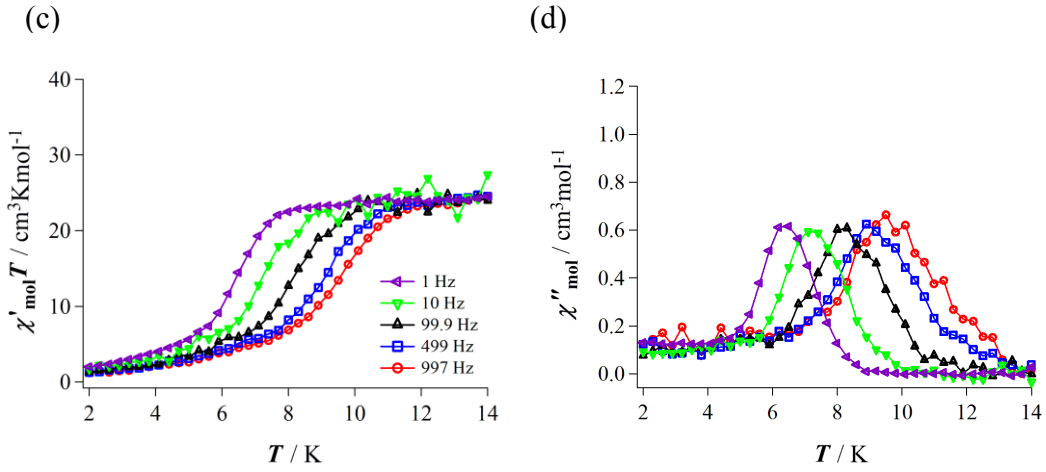

Fig. 5. $\chi'_{mol}T$ vs. T and χ''_{mol} vs. T plots for **1c** (a and b) and **2c** (c and d) with a 3.9 Oe ac field oscillating at given frequencies, The solid lines are a visual guide.

The value of $\Delta T_f/T_f(0)\Delta(\log w)$, where ΔT_f is the shift of the peak-temperature in χ'_{mol}, $\log w$ is the logarithm of the applied frequency, and $T_f(0)$ is the position of the peak at zero frequency was used for the evaluation of the complex showing slow magnetic relaxation. The values obtained from the χ'_{mol} vs. T plots for **1c** and **2c** were 0.24 and 0.24, respectively. According to Mydosh's work [11], those values are in the region $\Delta T_f/T_f(0)\Delta(\log w) > 0.2$ for an SMM and supports the formation of an SMM.

*3.2.3.2. dc magnetization decays measurements for **1c** and **2c***

To investigate the QTM pathway in the low temperature region, furthermore, the dc magnetization decays for **1c** and **2c** were measured after cycles of applying 50 kOe and then reducing to zero field. The decays of dc magnetizations, M_{mol}, were followed at various temperatures (5.0 – 1.9 K) in the period of 7 x 10^3 sec (ca. 2 hr). The data of M normalized by M_0; M at t = 0, for **1c** and **2c** were plotted as a function of time, t, and are shown in Fig. 6. On cooling from 5 K, the magnetization decay become slow and nearly reached the constant value of ~ 10^5 sec below 2.5 K, suggesting that QTM is the dominant pathway of the relaxation below 2.5 K. The temperature of 2.5 K is closed to the one at which the H_c and M_r values became constant in H_c and M_r vs. T plots (inset of Fig. 4).

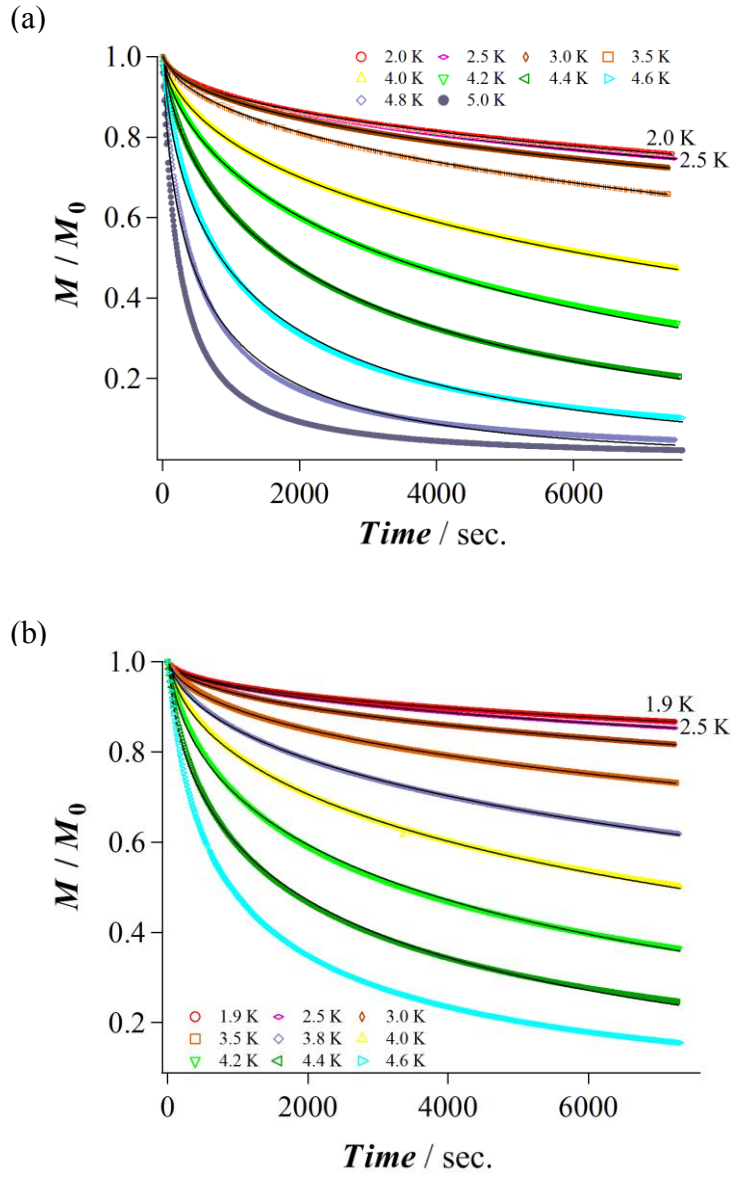

Fig. 6. M/M_0; M_0 is M at $t = 0$, vs. *time* plots for **1c** (a) and **2c** (b) at given temperatures. The solid lines indicate the fitting results (see in the text),

Data of dc magnetization decay at given temperatures were analyzed by a stretched exponential decay (equation 1) [12].

$$M = \ln(M_0)\text{-}(t/\tau)^B \qquad (1)$$

where M_0 is the initial magnetization, τ is the average relaxation time, and B is the width of the distribution; $B = 1$ is a single-exponential decay. Taking into account the magnitude of the M_0 value ($M_0(T)$; M_0 at T, $> 0.5M_0$ (1.9 or 2.0 K)), in which the values of $M_0(2.0)$ for **1c** and $M_0(1.9)$ for **2c** were 72 and 67 %, respectively, of M value at 50 kOe, the experimental decay data were selected and the data between 2.0 and 4.8 K for

1c and between 1.9 and 4.4 K for **2c** were used for the fitting experiments. The τ values of 5.6 x 10^2 – 1.1 x 10^5 and 2.8 x 10^3 – 5.4 x 10^5 sec with the *B*values of 0.45 – 0.58 and 0.44 – 0.49 for **1c** and **2c**, respectively, were obtained. The fitting results are listed in Table 3 and are shown by solid lines in Fig. 6.

Table 3

Values of τ and *B* for **1c** and **2c** at various temperatures.

T/K	τ / sec	
	1c	**2c**
1.9		5.4 x 10^5 (0.44)
2.0	1.1 x 10^5 (0.45)	
2.5	9.3 x 10^4 (0.46)	3.6 x 10^5 (0.46)
3.0	7.1 x 10^4 (0.47)	2.0 x 10^5 (0.46)
3.5	3.8 x 10^4 (0.50)	7.5 x 10^4 (0.47)
3.8		2.8 x 10^4 (0.49)
4.0	1.2 x 10^4 (0.53)	1.3 x 10^4 (0.48)
4.2	5.9 x 10^3 (0.58)	6.0 x 10^3 (0.48)
4.4	2.9 x 10^3 (0.55)	2.8 x 10^3 (0.45)
4.6	1.3 x 10^3 (0.52)	
4.8	5.6 x 10^2 (0.49)	

To compare with the τ values for **1c** and **2c,** the dc magnetization decays for the isomorphous complex, **3c**, were also measured in the range of 1.9 – 4.4 K under the similar condition. The dc decays were fast even at 1.9 K. The value of M_0(1.9) was 4.3 x 10^{-3} cm^3Oe, which was 26 % of the *M* value at 50 kOe. The decay data at 1.9, 2.1, and 2.4 K were used and τ values of 8.1 x 10^2, 6.5 x 10^2, and 5.8 x 10^2 sec with B = 0.39, 0.38, and 0.44, at 1.9, 2.1, and 2.4 K, respectively, were obtained. (Fig. S4)

*3.2.3.3. Decay time vs. T plots for **1c**, **2c**, and **3c***

The decay data obtained from both ac and dc experiments for **1c** and **2c** were combined and plotted as a function of inverse *T*, which are shown in Fig. 7. The relaxation times, τ, collected by the ac magnetic susceptibility technique and the dc magnetization decay measurements are clearly distinguishable. As shown by the solid line in Fig. 7, the magnetic relaxation time data obtained from ac measurements linearly increased on

cooling. From the Arrhenus plots; $\tau = 1/2\pi\nu = \tau_0 \exp(U_{eff}/k_B T)$, the activation energy, U_{eff}, for reorientation of the magnetic moment and the pre-exponential factor, τ_0, were estimated to be 139 and 135 K and 1.6 x 10^{-10} and 1.3 x 10^{-10} sec for **1c** and **2c**, respectively. In addition to the Mydosh's values ($\Delta T_f/T_f(0)\Delta(\log w) = 0.24$ for **1c** and **2c**), the strong frequency dependences of the χ'_{mol} and χ''_{mol} signals and the physically reasonable values of τ_0 also suggest that these carbene-Co(II) complexes function as SMM rather than spin glass [13]. In contrast, the relaxation times, τ, obtained by dc measurements gradually deviated from the linear line on cooling and reached a nearly constant value below 2.5 K, indicating that the decay predominantly took place in the QTM pathway. The values of lifetime, τ_Q, for QTM estimated from the temperaature –independent dc decay were 1.1 x 10^5 and 5.4 x 10^5 sec for **1c** and **2c**, respectively, which correspond to the half-life time, $t_{1/2}$, of 21 and 104 hr. Observed τ_Q might be due to the resonant quantum tunneling between $m_s = \pm 10/2$ [3].

To investigate the contribution of QTM pathway to the dc decay at 1.9 K for **3c**, it's Arrhenius plot [6] of ac data and the τ values at 1.9, 2.1, and 2.4 K were appended in Fig. 7a. As shown in Fig. 7a, the τ values at three temperatues were nearly constant and the value at 1.9 K largely deviated from the linear Arrhenius plot and was 8.3 x 10^5 times smaller than the value obtained from the extrapolation of Arrhenius plot at 1.9 K, indicating that the relaxation time at 1.9 K was strongly affected by QTM pathway. The value of 8.1 x 10^2 sec at 1.9 K was assigned as τ_Q for **3c**.

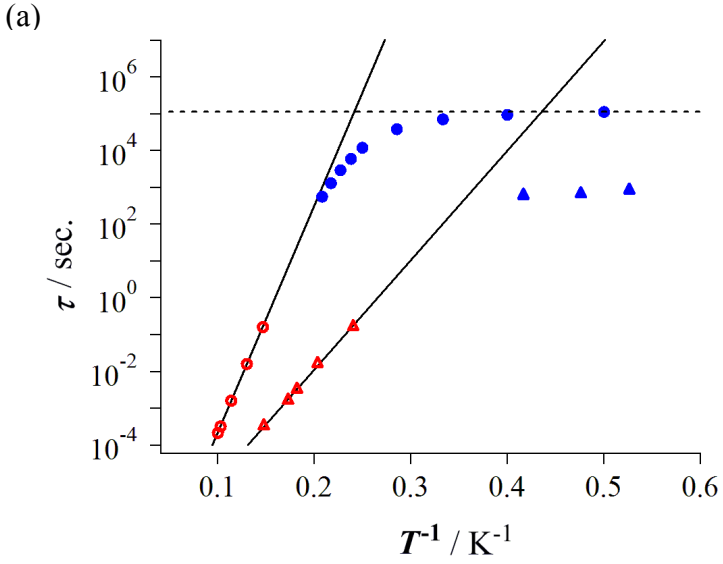

(b)

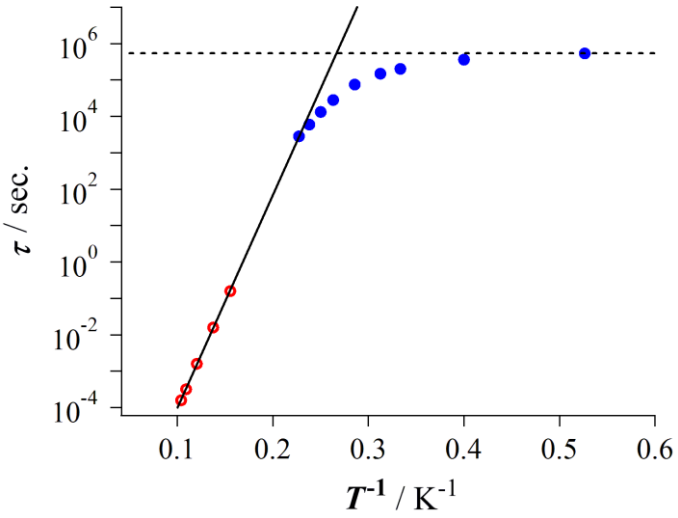

Fig. 7. τ vs. $1/T$ plots of the data obtained by ac (○) and dc (●) measurements for **1c** (a) and **2c** (b). Arrhenius plot and the τ values at 1.9, 2.1, and 2.4 K for **3c** (triangle) were appended in (a). The solid and broken lines indicate the fitting result of Arrhenius plot and the τ_Q value of QTM, respectively.

The magnetic behaviors observed after irradiation of **1** and **2** are reproducible. In annealing at 70 K, **3c** showed the increase in U_{eff} and H_c values, [6] while **1c** and **2c** had no appreciable change (U_{eff} = 135 and 131 K and H_c = 25 and 15 kOe for **1c** and **2c**). In annealing at 100 K, on the other hand, the observed SMM behaviors disappeared by chemical decomposition of carbene and returned to the magnetic behaviors before irradiation. This result clearly indicates that the magnetic interaction between the carbene center and the cobalt ion produces the SMM.

4. Conclusion

The cyclic dinuclear complexes, **1c** and **2c**, showed typical SMM behaviors with U_{eff} = 139 and 135 K and H_c = 26 and 15 kOe at 1.9 K, respectively. It is worthy to note that those U_{eff} values are the largest in the ones for SMM reported in the literatures and the values of the quantum tunneling time, τ_Q, for **1c** and **2c**, could be determined to be 1.1 x 10^5 and 5.4 x 10^5 sec ($t_{1/2}$ = 21 and 104 hours), respectively. The molecular structure for complexes, **1** and **2**, and their SMM properties after irradiation were compared with those for **3** reported previously. Three complexes had isomorphous structures and

functioned as SMM after irradiation. However, the SMM properties for **1c** and **2c**, which were comparable to each other, were largely different from that (U_{eff} = 96 K and H_c = 10 kOe at 1.9 K) [6] for **3c**. Furthermore, the τ_Q values for **1c** and **2c** were ~ 10^5 sec, while the lifetime of QTM for **3c** was much short and the τ_Q values was estimated to be 8.1 x 10^2 sec. From the results of SMM properties for three complexes, the electronic effect of substituents [14] on SMM properties might be insignificant. The observed differences of U_{eff} and τ_Q suggested that in these heterospin SMMs, the magnitude of U_{eff} and the rate of τ_Q were closely related and the slow τ_Q might be considered to lead large U_{eff}. [1, 3(a), 15] However, the relation between the U_{eff} and τ_Q in the heterospin SMM was not clarified by the present study. More detailed studies in the 2:2 cobalt complexes are in progress.

5. Supplementary materials

CCDC No. 803425, 734081, and 803858 for **D2py$_2$(TBA)**, **1** and **2**, respectively, contain the supplementary crystallographic data for this paper. These data can be obtained free of charge via http://www.ccdc.cam.ac.uk/conts/retrieving.html, or from the Cambridge Crystallographic Database Centre, 12 Union Road, Cambridge, CB2 1EZ, UK; Fax: (+44) 1223-336-033; or e-mail: deposit@ccdc.cam.ac.uk.

Acknowledgement.

This work was partially supported by "Nanotechnology Support Project" of the Ministry of Education, Culture, Sports, Science and Technology (MEXT), Japan. D.Y. acknowledges a scholarship by the Japan Society for the Promotion of Science (JSPS).

References

[1] D. Gatteschi, R. Sessoli, J. Villain, Molecular nanomagnets, Oxford University Press, 2006.

[2] (a) P. D. W. Boyd, Q. Li, J. B. Vincent, K. Folting, H-R. Chang, W. E. Streib, J. C. Huffman, G. Christou, D. N. Hendrickson, J. Am. Chem. Soc. 110 (1988) 8357;

(b) A. Caneschi, D. Gatteschi, R. Sessoli, J. Am. Chem. Soc. 113 (1991) 5873;
(c) C. Boskovic, E. K. Brechin, W. E. Streib, K. Folting, J. C. Bollinger, D. N. Hendrickson, G. Christou, J. Am. Chem. Soc. 124 (2002) 3725;
(d) J. Yoo, W. Wernsdorfer, E-C. Yang, M. Nakano, A. L. Rheingold, D. N. Hendrickson, Inorg. Chem. 44 (2005) 3377;
(e) N. Ishikawa, M. Sugita, W. Wernsdorfer, J.Am. Chem. Soc. 127 (2005) 3650;
(f) C. J. Milios, R. Inglis, A. Vinslava, R. Bagai, W. Wernsdorfer, S. Persons, S. P. Perlepes, G. Christou, E. K. Brechin, J. Am. Chem. Soc. 129 (2007) 12505;
(g) P-H. Lin, T. J. Burchell, L. Ungur, L. F. Chibotaru, W. Wernsdorfer, M. Murugesu, *Angew. Chem. Int. Ed*. 48 (2009) 9489;
(h) G. Abbas, Y. H. Lan, G. E. Kostakis, W. Wernsdorfer, C. E. Anson, A. K. Powell, Inorg. Chem. 49 (2010) 8067;
(i) E. Riviere, B. Donnio, E. Voirin, G. Rogez, J. P. Kappier, J. L. Gallani, *J. Mater. Chem*. 20 (2010) 7165;
(j) D. M. Pajerowski, T. C. Stamatatos, S. Mukherjee, E. S. Knowies, M. Bencomo, M.V. V. Meisei, G. Christou, Polyhedron. 29 (2010) 2462;
(k) Y-Z. Zhang, B-W. Wang, O. Sato, S. Gao, Chem. Commun. 46 (2010) 6959.

[3] (a) L. Lecren, W. Wernsdorfer, Y. G. Li, O. Roubeau, H. Miyasaka, R. Clerac, J. Am. Chem. Soc. 127 (2005) 11311;
(b) N. E. Chakov, S-C. Lee, A. G. Harter, P. L. Kuhns, A. P. Reyes, S. O. Hill, N. S. Dalal, W. Wernsdorfer, K. A. Abboud, G. Christou, J. Am. Chem. Soc. 128 (2006) 6975;
(c) C. J. Milios, A. Vinslava, P. A. Wood, S. Parsons, W. Wernsdorfer, G. Christou, S. P. Perlepes, E. K. Brechin, J. Am. Chem. Soc. 129 (2007) 8;
(d) C. J. Milios, A. Vinslava, W. Wernsdorfer, S. Moggach, S. Parsons, S. P. Perlepes, G. Christou, E. K. Brechin, J. Am. Chem. Soc. 129 (2007) 2754.

[4] N. Koga, S. Karasawa, Bull. Chem. Soc. Jpn. 78 (2005) 1384.

[5] (a) S. Karasawa, G. Zhou, H. Morikawa, N. Koga, J. Am. Chem. Soc. 125 (2003) 13676;
(b) H. Tobinaga, M. Suehiro, T. Ito, G. Zhou, S. Karasawa, N. Koga, *Polyhedron*. 26 (2007) 1905;
(c) S. Karasawa, D. Yoshihara, M. Nakano, N. Koga, Dalton Trans. (2008) 1418;

(d) S. Kanegawa, S. Karasawa, M. Maeyama, M. Nakano, N. Koga, J. Am. Chem. Soc. 130 (2008) 3079.

[6] D. Yoshihara, S. Karasawa, N. Koga, J. Am. Chem. Soc. 130 (2008) 10460.

[7] (a) *SIR 92*: A. Altomare, M. C. Burla, M. Camalli, M. Cascarano, C. Giacovazzo, A. Guagliardi, G. Polidori, J. Appl. Cryst. 27 (1994) 435;
(b) *DIRDIF99*: P. T. Beurskens, G. Admiraal, G. Beurskens, W. P. Bosman, R. de Gelder, R.Israel, J. M. M. Smits, The DIRDIF-99 program system, Technical Report of the Crystallography Laboratory, University of Nijmegen, The Netherlands. 1994;
(c) *Crystal Structure 3.5.1* : Crystal Structure Analysis Package, Rigaku and Rigaku/MSC, 2000-2003, 9009 New Trails Dr. The Woodlands TX 77381 USA.

[8] O. Kahn, Molecular Magnetism, Wiley-VCH Publishers, Weinheim, 1993.

[9] Y-H. Liu, Y-C. Cheng, Y-L. Tung, Y. Chi, T-L. Chen, C-S. Iiu, S-M. Peng, G. H. Lee, J. Mater. Chem. 13 (2003) 135.

[10] (a) H. Sakiyama, R. Ito, H. Kumagai, K. Inoue, M. Sakamoto, Y. Nishida, M. Yamasaki, Eur. J. Inorg. Chem. (2001) 2027;
(b) J. M. Herrera, A. Bleuzen, Y. Dromzee, M. Julve, F. Lloret, M Verdaguer, Inorg. Chem. 42 (2003) 7052.

[11] J. A. Mydosh, Spin Glasses; An Experimental Introduction, Taylor and Francis, London, 1993.

[12] (a) L. Thomas, A. Caneschi, B. Barbara, Phys. Rev. Lett, 83 (1999) 2398; (b) S. M. J. Aubin, Z. Sun, L. Pardi, J. Krzystek, J. Folting, L-C. Brunel, A. L. Rheingold, G. Christou, D. N. Hendrickson, Inorg. Chem, 38 (1999) 5329; (c) D. N. Hendrickson, G. Christou, H. Ishimoto, Y. Yoo, E. K. Brechin, A. Yamaguchi, E. M. Rumberger, S. M. J. Aubin, Z. Sum, G. Aromi, Polyhedron. 20 (2001) 1479.

[13] (a) S. P. Sellers, B. J. Korte, J. P. Fitzgerald, W. M. Reiff, G. Yee, J. Am. Chem. Soc. 120 (1998) 4662;
(b) M. A. Gî rtu, C. M. Wynn, W. Fujita, K. Awaga, A. J. Epstein, Phys. Rev. B. 61 (2000) 4117;

(c) E. Pardo, P. Burguete, R. Ruiz-García, M. Julve, D. Beltrán, Y. Journaux, P. Amorós, F. Lloret, J. Mater. Chem. 16 (2006) 2702.

[14] (a) T. Ikeue, Y. Ohgo, T. Saitoh, T. Yamaguchi, M. Nakamura, Inorg Chem, 40 (2001) 3423, (b) A. Ikezaki, T. Ikeue, M. Nakamura, Inorg. Chim. Acta. 335 (2002) 91.

[15] C. Sangregorio, T. Ohm, C. Paulsen, R. Sessolo, D. Gateschi. Phys. Rev. Lett. 78 (1997**)** 4645.